In-room Reverberant Multi-link Channels: Preliminary Investigations

TD(12)03042

Steinböck, Gerhard; Pedersen, Troels; Fleury, Bernard Henri; Wang, Wei; Raulefs, Ronald

Publication date:
2012

Document Version
Early version, also known as pre-print

EUROPEAN COOPERATION
IN THE FIELD OF SCIENTIFIC
AND TECHNICAL RESEARCH

EURO-COST

SOURCE: Aalborg University

IC1004 TD(12)03042
Barcelona, Spain
February 8-10, 2012

In-room Reverberant Multi-link Channels: Preliminary Investigations

G. Steinböck, T. Pedersen, B.H. Fleury
Aalborg University
Dept. of Electronic Systems
Section NavCom
Fredrik Bajers Vej 7C
DK-9220 Aalborg East
DENMARK

W. Wang, R. Raulefs
German Aerospace Center (DLR)
Institute of Communications and Navigation
Oberpfaffenhofen
D-82234 Wessling
GERMANY

Phone: +45 9815 8615
Fax: +45 9815 1583
Email: gs@es.aau.dk

In-room Reverberant Multi-link Channels: Preliminary Investigations

Gerhard Steinböck, Troels Pedersen
and Bernard H. Fleury
Dept. of Electronic Systems,
Section Navigation and Communications,
Aalborg University
Fredrik Bajers Vej 7, DK-9220 Aalborg East, Denmark
Email: {gs, troels, bfl}@es.aau.dk

Wei Wang and Ronald Raulefs

Institute of Communications and Navigation,
German Aerospace Center (DLR)
Oberpfaffenhofen, 82234 Wessling, Germany
Email: {wei.wang, ronald.raulefs}@DLR.de

***Abstract*—We model the delay power spectrum of in-room reverberant multi-link radio channels. The model relies on the empirical observation that the delay power spectrum of each link measured in a closed room, consists of an early peak and a late exponential reverberation tail. The peak vanishes as the transmitter-receiver distance increases; the exponential decay of the reverberation tail is invariant with distances, while the onset of the tail is equal to the propagation time between the transmitter and the receiver. The proposed model allows for the prediction of path loss, mean delay, and rms delay spread versus distance for multiple links. These predictions are in good agreement with the estimates obtained from the multi-link measurements.**

I. Introduction

The field of indoor radio-localization has recently attracted significant interest. One approach for solving the localization problem is to rely on the measured power of the received signal [1] and to use a path loss model to infer the corresponding length of a radio link. Knowledge of the received power is often used for localization in already deployed systems (e.g. WiFi) where received signal strength is readily available or with cheap low power devices in sensor networks. To obtain an ambiguity free location estimate, multiple transmitter-receiver distance estimates are necessary. Thus multi-link models are of importance for radio-localization purposes.

In [2] we propose a distance dependent delay power spectrum model for in-room reverberant channels. This model builds on experimental observations of the behavior of the delay-power spectrum [3], [4] and on analogies to models used in room acoustics [5] and electromagnetic fields in cavities [6]. The model of the delay-power spectrum consists of a dominant and a reverberant component, which both depend on distance. This allows for the prediction of path gain (inverse of path loss), mean delay and rms delay spread versus distance. Thus, the model can be used to predict the transmitter-receiver distance based on measurement of one of these quantities, e.g. for localization purpose.

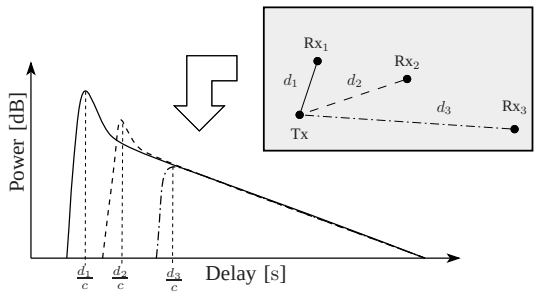

Fig. 1. Typical behavior of the bandlimited delay-power spectrum experimentally observed in an in-room environment at three different transmitter-receiver distances (schematically presented by the grey box).

In this contribution we present preliminary results on the delay power spectrum model used in a multi-link scenario. We summarize the model and validate it by comparing the predicted received power, mean delay and rms delay spread with estimates obtained from multi-link measurements.

II. Delay Power Spectrum Model

As in [2], we consider an in-room scenario as illustrated in Fig. 1. The delay-power spectrum is observed at different transmitter and receiver locations. A system bandwidth high enough to observe frequency fading (delay dispersion), but too low to separate single propagation paths in the environment is considered. The considered carrier frequencies are high enough, such that the smallest dimension of the room is large compared to the wavelength λ. The delay-power spectrum is the expectation of the squared magnitude of the impulse response $h(\tau, d)$:

$$G(\tau, d) = \mathrm{E}[|h(\tau, d)|^2]. \quad (1)$$

Here τ is the delay and d is the transmitter-receiver distance. In [4] it is observed that the delay-power spectrum in such an in-room scenario exhibits the typical

TABLE I
PARAMETERS OF THE PROPOSED MODEL.

Parameter	Meaning
G_0	Path gain at reference distance d_0.
d_0	Reference distance, typically 1 m.
n	Path gain decay exponent of the dominant component.
q	Ratio $G_{\mathrm{rev}}(d_0)/G_{\mathrm{dom}}(d_0)$.
T	Reverberation time of the reverberant component.

behavior depicted in Fig. 1. The tail of the delay-power spectrum exhibits the same constant exponential decay regardless of the transmitter-receiver distance. The early part is strong at short distance and gradually vanishes as the distance increases.

Based on these observations, we model the delay-power spectrum as a dominant component plus a reverberant component:

$$\begin{aligned} G(\tau, d) &= \mathrm{E}[|h_{\mathrm{dom}}(\tau, d)|^2] + \mathrm{E}[|h_{\mathrm{rev}}(\tau, d)|^2] \\ &= G_{\mathrm{dom}}(\tau, d) + G_{\mathrm{rev}}(\tau, d). \end{aligned} \tag{2}$$

Subscript dom indicates the dominant component and subscript rev denotes the reverberant component. The dominant component represents the early part of the delay-power spectrum consisting of a directly propagating component and possible first-order reflections from the floor, ceiling and walls. The reverberant component represents the multitude of higher order reflections in the room which yield the diffuse tail of the delay-power spectrum.

We model the delay-power spectrum of the dominant component as

$$G_{\mathrm{dom}}(\tau, d) = G_0 \left(\tfrac{d_0}{d}\right)^n \delta\left(\tau - \tfrac{d}{c}\right), \tag{3}$$

where n is the power decay exponent, $\delta(\,\cdot\,)$ is the Dirac delta function, c the speed of light, and $G_0 > 0$ is the gain at the reference distance d_0.

We model the reverberant delay-power spectrum as an exponentially decaying function with onset equal to the propagation time between the transmitter and the receiver:

$$G_{\mathrm{rev}}(\tau, d) = \begin{cases} G_{0,\mathrm{rev}}\, e^{-\frac{\tau}{T}}, & \tau > \frac{d}{c} \\ 0, & \text{otherwise} \end{cases} \tag{4}$$

where $G_{0,\mathrm{rev}}$ is the reference gain of the reverberant component. In analogy to acoustics [4], [5] we call T the reverberation time.

III. PREDICTIONS OF THE DELAY POWER SPECTRUM MODEL

Based on the model (2) we derived in [2] expressions for the path gain, mean delay, and rms delay spread as a function of the transmitter-receiver distance.

A. Path gain

The path gain at distance d is

$$\begin{aligned} G(d) &= \int G(\tau, d)\mathrm{d}\tau \\ &= \underbrace{G_0 \left(\tfrac{d_0}{d}\right)^n}_{G_{\mathrm{dom}}(d)} + \underbrace{G_{0,\mathrm{rev}}\, T\, e^{\frac{-d}{c\,T}}}_{G_{\mathrm{rev}}(d)}. \end{aligned} \tag{5}$$

The component $G_{\mathrm{dom}}(d)$ decays with d^{-n}, while $G_{\mathrm{rev}}(d)$ decays exponentially. Denoting by q the ratio of reverberant to dominant gain at reference distance d_0:

$$q = \frac{G_{\mathrm{rev}}(d_0)}{G_{\mathrm{dom}}(d_0)} = \frac{G_{0,\mathrm{rev}}}{G_0}\, T\, e^{\frac{-d_0}{c\,T}}, \tag{6}$$

the path gain can be recast as

$$G(d) = G_0 \left(\tfrac{d_0}{d}\right)^n + G_0\, q\, e^{\frac{d_0 - d}{c\,T}}. \tag{7}$$

The graph of $G(d)$ versus distance and q as parameter is depicted in Fig. 2a. At small distances $G_{\mathrm{dom}}(d)$ dominates and the path gain decays as d^{-n}. Beyond the reverberance distance d_r, the contribution of the reverberant component $G_{\mathrm{rev}}(d)$ in $G(d)$ leads to a deviation from $G_{\mathrm{dom}}(d)$.

The standard path gain model is a special case of (7) where the reverberant component is zero ($q = 0$). It reads

$$G_{\mathrm{std}}(d) = G_0 \left(\tfrac{d_0}{d}\right)^n. \tag{8}$$

We remark that the path loss is defined as the inverse of the path gain: $L(d) = G(d)^{-1}$. For notational convenience we consider only path gain in the sequel.

B. Mean Delay and Root Mean Squared Delay Spread

We derived the mean delay at distance d in [2] from (2) as

$$\mu_\tau(d) = \frac{1}{G(d)} \int \tau\, G(\tau, d)\mathrm{d}\tau \tag{9}$$

$$= \tfrac{d}{c} + T \frac{1}{1 + \left(\tfrac{d_0}{d}\right)^n \tfrac{1}{q}\, e^{\frac{d - d_0}{c\,T}}}. \tag{10}$$

In (10) the first term is the delay of a directly propagating component and the second term results from the reverberant component. Fig. 2b depicts the mean delay versus distance with the settings specified in the figure. The mean delay increases with distance. For distances larger than the reverberance distance, the curves approximately follow the straight line $\frac{d}{c} + T$.

Similarly the rms delay spread reads:

$$\sigma_\tau^2(d) = \frac{1}{G(d)} \int \tau^2\, G(\tau, d)\mathrm{d}\tau - \left(\mu_\tau(d)\right)^2, \tag{11}$$

$$= \frac{T^2}{1 + \left(\tfrac{d_0}{d}\right)^n \tfrac{1}{q}\, e^{\frac{d - d_0}{c\,T}}} \left(2 - \frac{1}{1 + \left(\tfrac{d_0}{d}\right)^n \tfrac{1}{q}\, e^{\frac{d - d_0}{c\,T}}}\right). \tag{12}$$

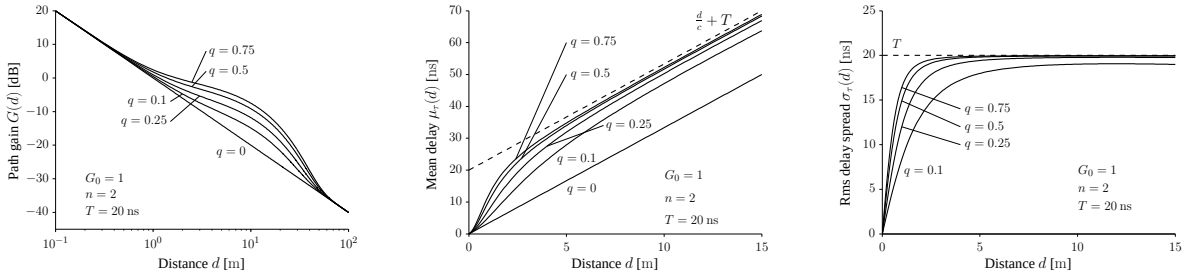

(a) (b) (c)

Fig. 2. Path gain (a), mean delay (b) and rms delay spread (c) versus distance predicted by the proposed model for $d_0 = 1$ m.

Fig. 2c depicts the rms delay spread versus distance. For distances larger than the reverberance distance $\sigma_\tau(d)$ approaches the reverberation time T.

C. Extension to the Multi-link Scenario

In the multi-link case we make use of the assumption that the delay power spectrum model and the corresponding model parameter settings are the same for all positions in the room. The dominant and reverberant component depend solely on the transmitter-receiver distance. Then for link k with transmitter-receiver distance d_k we have path gain $G(d_k)$, mean delay $\mu(d_k)$ and rms delay spread $\sigma(d_k)$.

IV. Measurement Setup

We validate the proposed model by means of measurement data from a campaign [7] conducted at DLR in Oberpfaffenhofen, Germany. The investigated room is sketched in Fig. 3. A panograph of it is depicted in Fig. 4. During the measurement process the environment was static and no one was in the room.

The room dimensions are $5.1 \times 5.25 \times 2.78\,\mathrm{m}^3$. The three inner walls are made of plaster boards. As visible in the panograph, the outer "wall" consists mainly of four windows (W1–W4) and two pillars made of concrete. The frames of the windows are metallic and the glass is metal coated. The height of the transmit and receive antenna was 1.26 m and 1.1 m, respectively.

The measurement data were collected using the Rusk-DLR channel sounder [8] operating at 5.2 GHz with a bandwidth of 120 MHz. The transmit antenna [9] was omni-directional with 3 dBi gain. A uniform circular array of eight monopoles with diameter 75.18 mm was used at the receiver. The transmitter and receiver were synchronized to a common clock via cables throughout the measurements.

The receive antenna array was placed at five fixed locations labeled as Rp1 to Rp5 respectively in Fig. 3. The transmit antenna was mounted on a model train which moved on two tracks labeled as T1 and T2. Frequency responses were measured for each receiver

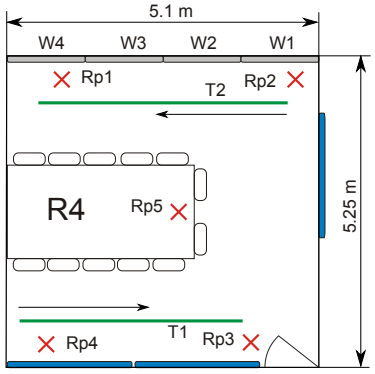

Fig. 3. Schematic of the investigated room. The arrows next to the tracks indicate the transmitter movement direction.

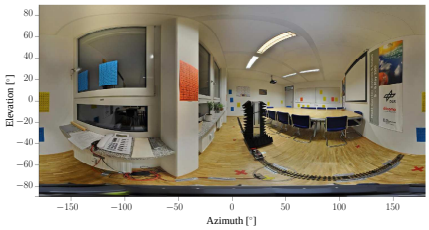

Fig. 4. Panograph (spherical panoramic photo) of the investigated room seen from Rp1 using an equi-rectangular projection.

position while the transmitter was moving along the two tracks.

The positions Rp1-Rp5 and the trajectories along the tracks were measured with a tachymeter. The odometer of the model train was connected to the channel sounder to record the traveled distance.

V. Model Fitting and Validation

A. Measurement Post Processing and Model Parameter Estimation

In this contribution we only consider the measurements obtained for receiver positions Rp1 to Rp4 and the transmitter moving on both, tracks T1 and T2. We compute the received power and the delay power spectrum at all pairs of transmitter-receiver positions as described

TABLE II
PARAMETER ESTIMATES FOR THE STANDARD AND PROPOSED MODELS.

Model	$\widehat{G}_0$	$\widehat{n}$	$\widehat{q}$	$\widehat{T}$ [ns]
Standard	$1.14 \cdot 10^{-5}$	1.13	—	—
Proposed	$6.85 \cdot 10^{-6}$	2.2	0.54	18.4

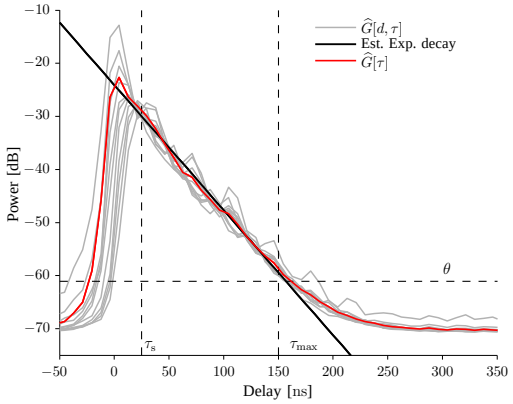

Fig. 5. Spatially averaged delay-power profiles obtained for transmitter-receiver distance intervals of 4λ for receiver positions Rp1 to Rp4 when the transmitter was moving along track T1 and T2. For clarity reasons only the delay power profiles of every second distance interval are shown. The straight line depicts an exponentially decaying function with decay factor $\widehat{T} = 18.4\,\text{ns}$. The dashed lines indicate the range $\tau_s = 25\,\text{ns} \leq \tau \leq \tau_{\max} = 150\,\text{ns}$ used for the estimation of $\widehat{T}$.

in detail in [2]. Fig. 6 reports the scatter plot of power values versus transmitter-receiver distance. As can be seen in Fig. 5 the underlying model assumption (4) holds true for the experimental delay-power spectra. Using the method, detailed in [2], to estimate the reverberation time in the range $25\,\text{ns} \leq \tau \leq 150\,\text{ns}$ yields $\widehat{T} = 18.4\,\text{ns}$.

We fit both the standard path loss model (8) and the proposed model as detailed in [2]. The estimates of the parameters of the models are reported in Table II and the path gains versus distance computed from the models with these parameter settings are shown in Fig. 6. For small distances the proposed model fits the estimated received power values better than the standard path gain model.

We compute the mean delay estimates $\widehat{\mu}_\tau$ and rms delay spread estimates $\widehat{\sigma}_\tau$ for each pair of transmitter-receiver positions from the estimates of the delay power spectra using (9) and (11), respectively. These estimates computed for all transmitter-receiver positions are reported for the multi-link scenario with the transmitter moving on track T1 in Fig. 9 and Fig. 10. These values are in accordance with values reported in [10] for office environments.

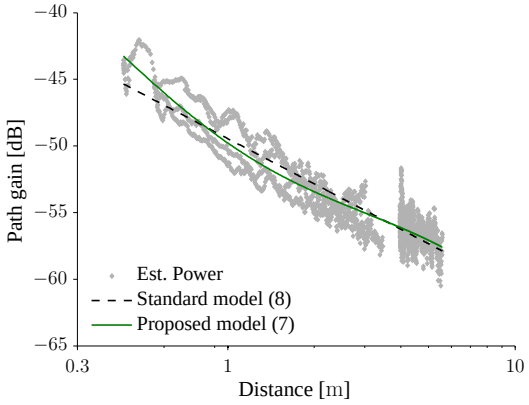

Fig. 6. Estimated received power versus distance with the predictions computed using the standard and the proposed path gain models.

B. Multi-link Preliminary Results

The transmitter-receiver distance between the multi-links and the model parameters reported in Table II are used to predict the path gain, mean delay and rms delay spread for the multi-links with (7), (10) and (12), respectively. Fig. 7 reports the transmitter-receiver distances when the transmitter is moving along track T1. We observe rather small changes in the transmitter-receiver distance for the receiver positions Rp1 and Rp2 (opposite T1). For Rp3 and Rp4 we observe a clear change in transmitter-receiver positions as in the one case the transmitter moves towards and in the other moves away from the receiver.

Fig. 8 shows model predictions of the received power together with the estimated receive power from the experimental data. The predictions of the standard and the proposed models are close to each other and follow well the trend of the received power estimates.

The proposed delay power spectrum model allows for the prediction of mean delay and rms delay spread. These predicted values are shown together with the estimates from the experimental results in Fig. 9 and 10. The trend of the obtained estimates from the experimental data follows closely the predictions. This is remarkable as for the model fitting we used only: i) an estimate of T from the exponential decay of the tail of the delay power spectrum and ii) the estimates of the received power versus transmitter-receiver distance.

VI. CONCLUSIONS

We propose a model for the delay power spectrum of in-room multi-link channels. The model is able to predict the received power, mean delay and rms delay spread in the multi-link case. We observe that the predictions of the model agree well with the trends observed in the estimates obtained from the measured data. These estimates

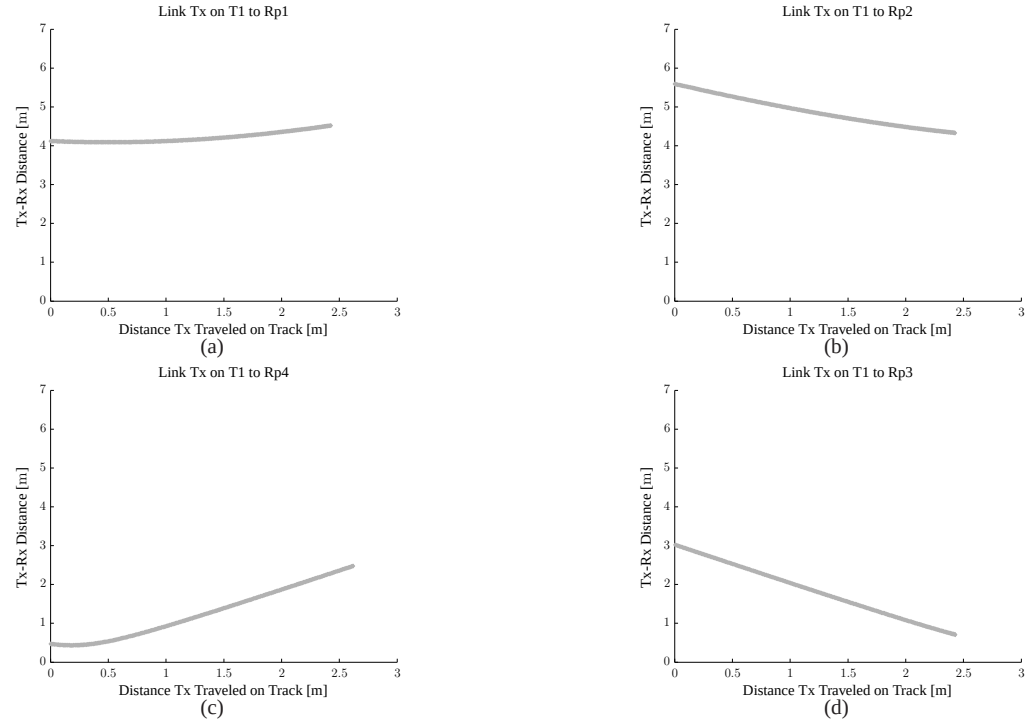

Fig. 7. Transmitter-receiver distance of the different links for the transmitter moving along track T1. The distance is obtained for the center of the receiver array.

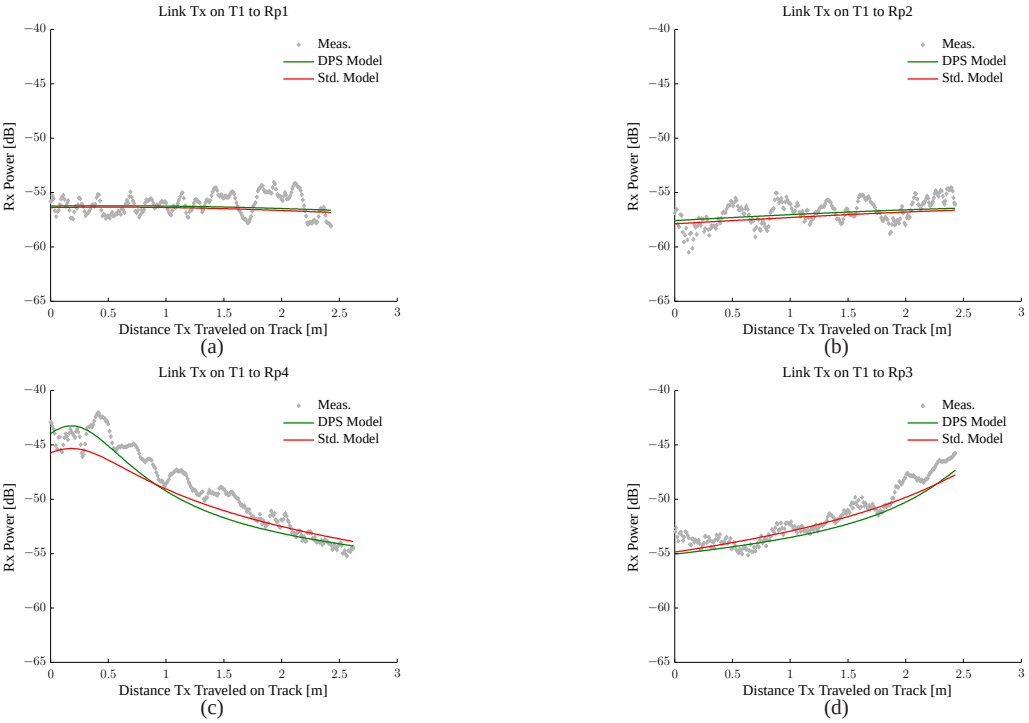

Fig. 8. Estimates of the received power from experimental data together with predictions for the multi-link scenario with the transmitter moving along track T1.

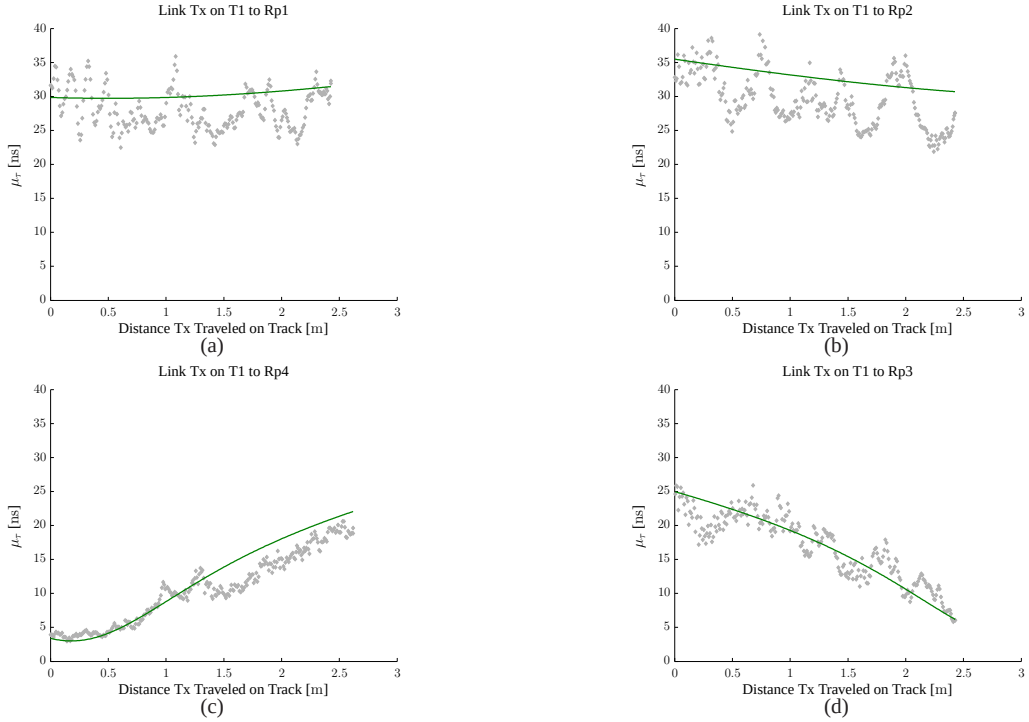

Fig. 9. Estimates of the mean delay from experimental data and the predictions in the multi-link case with the transmitter moving along track T1.

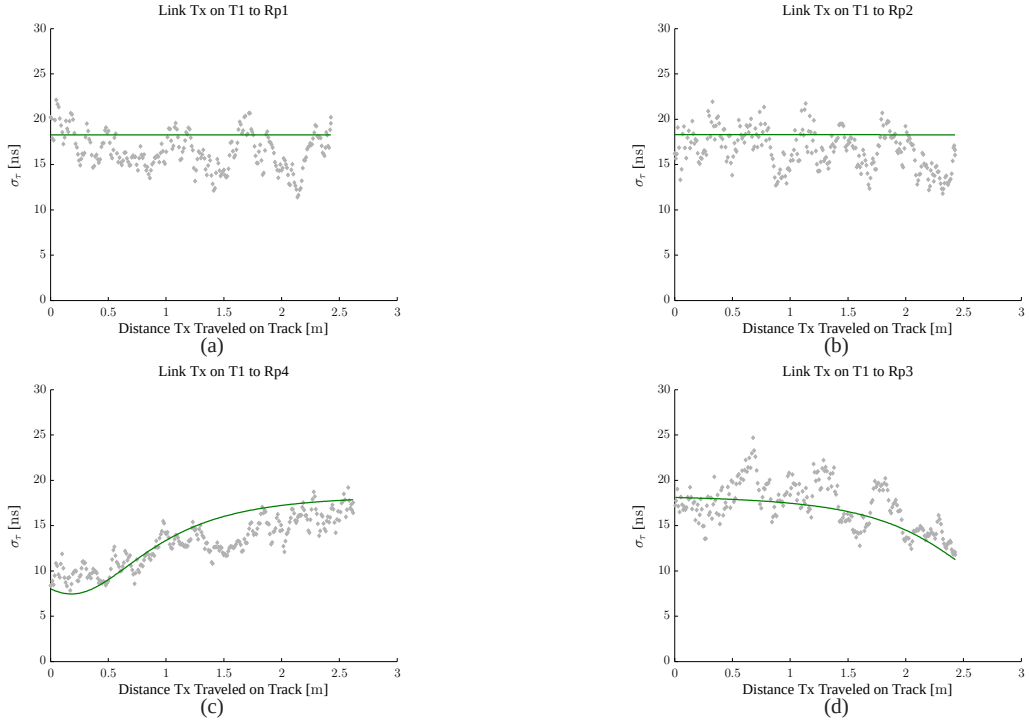

Fig. 10. Estimates of the rms delay spread from experimental data and the predictions in the multi-link case with the transmitter moving along track T1.

show a random fluctuation which can be attributed to small scale fading. In a next step we will include in the model these fluctuations. To that end the model should be extended to account for the correlation between the received power, mean delay and rms delay spread in both single and multi-link cases.

ACKNOWLEDGMENT

This work was supported by the project ICT-248894 Wireless Hybrid Enhanced Mobile Radio Estimators – Phase 2 (WHERE2).

REFERENCES

[1] H. Liu, H. Darabi, P. Banerjee, and J. Liu, "Survey of Wireless Indoor Positioning Techniques and Systems," *IEEE Trans. Syst., Man, Cybern. C*, vol. 37, no. 6, pp. 1067–1080, Nov. 2007.

[2] G. Steinböck, T. Pedersen, B. Fleury, W. Wang, T. Jost, and R. Raulefs, "Model for the Path Loss of In-room Reverberant Channels," in *Vehicular Technology Conference (VTC 2011-Spring), 2011 IEEE 73rd*, May 2011, pp. 1–5.

[3] C. Holloway, M. Cotton, and P. McKenna, "A model for predicting the power delay profile characteristics inside a room," *IEEE Trans. Veh. Technol.*, vol. 48, no. 4, pp. 1110–1120, 1999.

[4] J. B. Andersen, J. Ø. Nielsen, G. F. Pedersen, G. Bauch, and J. M. Herdin, "Room electromagnetics," *IEEE Antennas Propag. Mag.*, vol. 49, no. 2, pp. 27–33, 2007.

[5] H. Kuttruff, *Room Acoustics*, 4th ed. London: Taylor & Francis, 2000.

[6] D. A. Hill, *Electromagnetic Fields in Cavities: Deterministic and Statistical Theories*, ser. IEEE Press Series on Electromagnetic Wave Theory. Piscataway, NJ: Wiley/IEEE Press, 2009.

[7] G. Steinböck, T. Pedersen, and W. Wang, "AAU-DLR 2010 Indoor Measurement Campaign – Measurements for Validation of Models for Reverberant and Cooperative Channels," AAU and DLR, Report, 2011.

[8] J. Stephan, Y. Lostanlen, J. Keignart, W. Wang, D. Slock, and F. Kaltenberger, "Measurements of location-dependent channel features," ICT-217033 WHERE, Del. 4.1, Oct. 2008, http://www.ict-where.eu/.

[9] Huber+Suhner, "Datasheet for Sencity Antenna For In-Carriage Wireless Communication, Type: SOA 5600/360/3/20/V_1," Document No. 01.02.1358, May 2007.

[10] E. Damosso, Ed., *Digital mobile radio towards future generation systems: COST 231 Final Report*. Bruxelles, Belgium: European Commission, 1999.